Oxidative stress fuels *Trypanosoma cruzi* infection in mice

Claudia N. Paiva,[1] Daniel F. Feijó,[1] Fabianno F. Dutra,[1] Vitor C. Carneiro,[2] Guilherme B. Freitas,[1] Letícia S. Alves,[1] Jacilene Mesquita,[1] Guilherme B. Fortes,[1] Rodrigo T. Figueiredo,[3] Heitor S.P. Souza,[4] Marcelo R. Fantappié,[2] Joseli Lannes-Vieira,[5] and Marcelo T. Bozza[1]

[1]Laboratório de Inflamação e Imunidade, Departamento de Imunologia, Instituto de Microbiologia Professor Paulo de Góes (IMPPG), [2]Instituto de Bioquímica Médica, Programa de Biotecnologia e Biologia Molecular, [3]Instituto de Ciências Biomédicas, Pólo de Xérem, and [4]Hospital Universitário, Serviço de Hematologia, Universidade Federal do Rio de Janeiro (UFRJ), Rio de Janeiro, Brazil. [5]Laboratório de Biologia das Interações, Instituto Oswaldo Cruz, Fiocruz, Rio de Janeiro, Brazil.

Oxidative damage contributes to microbe elimination during macrophage respiratory burst. Nuclear factor, erythroid-derived 2, like 2 (NRF2) orchestrates antioxidant defenses, including the expression of heme-oxygenase–1 (HO-1). Unexpectedly, the activation of NRF2 and HO-1 reduces infection by a number of pathogens, although the mechanism responsible for this effect is largely unknown. We studied *Trypanosoma cruzi* infection in mice in which NRF2/HO-1 was induced with cobalt protoporphyrin (CoPP). CoPP reduced parasitemia and tissue parasitism, while an inhibitor of HO-1 activity increased *T. cruzi* parasitemia in blood. CoPP-induced effects did not depend on the adaptive immunity, nor were parasites directly targeted. We also found that CoPP reduced macrophage parasitism, which depended on NRF2 expression but not on classical mechanisms such as apoptosis of infected cells, induction of type I IFN, or NO. We found that exogenous expression of NRF2 or HO-1 also reduced macrophage parasitism. Several antioxidants, including NRF2 activators, reduced macrophage parasite burden, while pro-oxidants promoted it. Reducing the intracellular labile iron pool decreased parasitism, and antioxidants increased the expression of ferritin and ferroportin in infected macrophages. Ferrous sulfate reversed the CoPP-induced decrease in macrophage parasite burden and, given in vivo, reversed their protective effects. Our results indicate that oxidative stress contributes to parasite persistence in host tissues and open a new avenue for the development of anti–*T. cruzi* drugs.

Introduction

Oxidative stress is generated during acute Chagas disease and contributes to the tissue damage observed with this infection. *Trypanosoma cruzi*, the causative agent of Chagas disease, infects cardiomyocytes, alters their mitochondrial potential, and induces ROS (1). This overwhelms the antioxidant defenses and produces persistent oxidative stress (2–4). Free iron and heme are released from damaged muscle cells and may potentially contribute to oxidative stress (5) and inflammation (6, 7). Furthermore, macrophages are activated to produce ROS via respiratory burst during infection (8–10). Though ROS are detrimental to most pathogens, *T. cruzi* has highly effective antioxidant machinery that may potentially confer resistance to oxidative environments (11).

Antioxidant defenses orchestrated by the transcription factor NRF2 help maintain redox environments in cellular compartments, allowing them to perform tasks that require ROS at optimal concentrations, such as protein folding in the endoplasmic reticulum (12). Increased mitochondrial respiration and phagocyte respiratory burst are oxidative events that can overwhelm NRF2-dependent antioxidant defenses and lead to redox imbalance. The expression of the enzyme HO-1 is regulated by NRF2. This enzyme has antiapoptotic, anti-inflammatory, and anti-immunogenic capacities (13). HO-1 can shift the redox balance by degrading the pro-oxidant heme and increasing the amount of the antioxidant biliverdin and, subsequently, bilirubin, by-products of this reaction. Pro-oxidant Fe^{2+} is also produced by heme degradation, but it is safely disposed of through sequestration by ferritin or exiting the cell through ferroportin (13). HO-1 can also translocate to the nucleus and directly activate antioxidant mechanisms (14). Additionally, NADPH oxidase (NOX2), the enzyme responsible for macrophage oxidative burst, is a heme-protein, and its activity is greatly decreased by the reduction of heme availability with the induction of HO-1 (15).

Pathogens may be subjected to ROS-mediated oxidative damage during phagocyte burst; in addition, ROS can combine with NO to form highly lethal peroxynitrite. There are a few exceptions to the rule that ROS are detrimental to pathogen growth: antioxidant administration, as well as deficiency in NOX2, decrease pathogen burden in some viral infections (16–18), and ROS favor the growth of *Mycobacterium abscessus* inside macrophages (19). The expression of NRF2 target antioxidant genes is thus expected to weaken defenses against ROS-sensitive pathogens. In fact, HO-1 expression promotes liver infection by *Plasmodium berghei* and *Plasmodium yoelii* (20). However, HO-1 induction reduces viral burden in hepatitis B (21), hepatitis C (22), enterovirus-71 (17), and HIV (23) infections; mediates macrophage resistance to *Salmonella* serovar Typhimurium (24); and enhances bacterial clearance of *Enterococcus faecalis* (25). NRF2 induction also reduces infection with RSV (26), and *Nrf2*$^{-/-}$ mice are susceptible to *Pseudomonas aeruginosa* (27). Together, these results suggest that NRF2/HO-1 might participate in innate immunity, perhaps against pathogens that thrive in oxidative environments. Herein, we investigated the therapeutic effects of HO-1 induction in *T. cruzi* infection. Our results indicate that oxidative stress generated in response to *T. cruzi* infection contributes to maintenance of high parasite burdens.

Conflict of interest: The authors have declared that no conflict of interest exists.
Citation for this article: *J Clin Invest.* doi:10.1172/JCI58525.

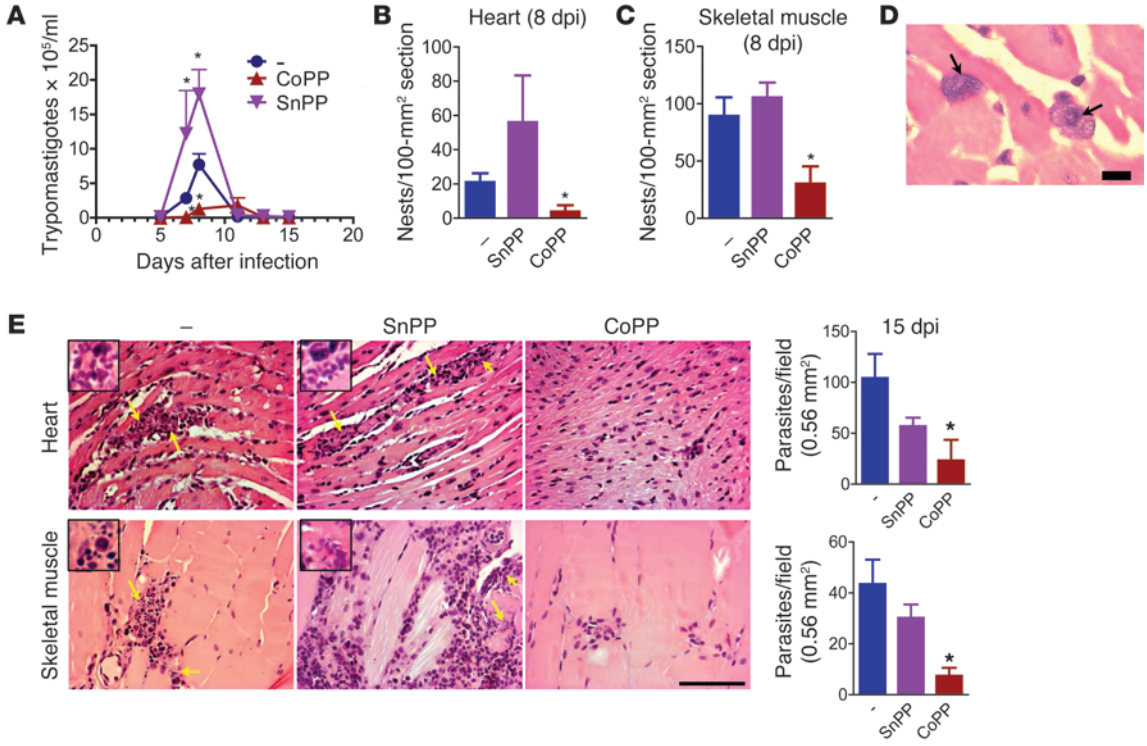

Figure 1
Treatment with CoPP reduces *T. cruzi* parasite burden. (**A**) Mean parasitemia during acute infection (n = 7 mice per time point). The experiment was performed 5 times. Mean parasitism in (**B**) heart and (**C**) skeletal muscle at 8 dpi. (**D**) Infected cells infiltrating the heart from SnPP-treated mice at 8 dpi. Scale bar: 10 μm. (**E**) Mean parasitism in heart and skeletal muscle at 15 dpi. At least 50 fields were assessed per H&E section from each of 4 mice per group. Yellow arrows indicate parasites. Insets (×560) show parasites among inflammatory leukocytes. Experiments were performed twice, with similar results. *P < 0.05 compared with infected nontreated controls. Error bars represent SEM. Scale bars: 100 μm.

Results

The NRF2/HO-1 inducer CoPP increases resistance to T. cruzi infection. To determine the role of HO-1 in acute *T. cruzi* infection, we infected C57BL/6 mice with the Y strain and treated them with cobalt protoporphyrin (CoPP), an inducer of HO-1 expression that activates NRF2 (28), or with tin protoporphyrin (SnPP), an inhibitor of HO-1 activity. Treatment was discontinued at the end of patent parasitemia (10 days after infection [dpi]). CoPP greatly reduced parasitemia, while SnPP increased it (Figure 1A). All mice survived infection with *T. cruzi*. At 8 dpi, parasitism was low in tissues from CoPP-treated mice but higher in hearts and skeletal muscle from SnPP-treated mice (Figure 1, B and C). Parasites were mostly confined to infiltrating cells in these tissues (Figure 1D). By 15 dpi, the parasitism was controlled in SnPP-treated mice, and CoPP-treated mice had reduced burden in the heart and striated muscle as compared with untreated controls (Figure 1E). Thus, contrary to our hypothesis, the induction of NRF2/HO-1 expression correlated with decreased parasite burden.

CoPP does not alter adaptive immunity. Both $CD8^+$ and Th1 lymphocytes are essential for controlling *T. cruzi* infection (29, 30). *T. cruzi* infection induces ROS production by macrophages, which inhibits the immunoproteasome and decreases class I antigen presentation (31). Based on that, we predicted that activating antioxidant mechanisms with CoPP treatment would favor MHC class I antigenic presentation and thus allow a more effective CD8-mediated protective response. However, treatment of $Cd8^{-/-}$ (Figure 2A) and perforin-knockout ($Pfn^{-/-}$) (Figure 2B) mice with CoPP reduced parasitemia and mortality to levels similar to those of wild-type mice.

Antioxidants alter Th responses (32). Treatment with CoPP did not alter the production of IFN-γ or IL-17A by splenocytes stimulated with ConA, anti-CD3, or *T. cruzi* antigen at 9 dpi (Figure 2C). IL-4 remained close to the lower limit of detection in all groups (data not shown). Plasma IFN-γ concentrations did not change in response to CoPP (Supplemental Figure 1A; supplemental material available online with this article; doi:10.1172/JCI58525DS1). Treatment of infected $Ifng^{-/-}$ mice with CoPP greatly reduced parasitemias and postponed death, although treatment did not totally compensate for their high susceptibility to infection. Infected $Ifng^{-/-}$ mice relapsed with parasitemia after treatment was discontinued at 10 dpi (Figure 2D). Likewise, treatment with CoPP greatly reduced parasitemia and postponed death of $Rag2^{-/-}$ mice, and parasitemia increased only after treatment was discontinued (Figure 2E). Also, CoPP did not substantially alter lymphocyte apoptosis (Supplemental Figure 1B). Together, these data indicate that CoPP does not reduce parasitism by regulating T lymphocyte immunity.

CoPP reduces macrophage parasitism in vivo and in vitro. Peritoneal macrophages from infected mice, untreated or treated with CoPP or SnPP, were screened for amastigotes at 9 dpi. Administration of CoPP to mice reduced macrophage parasitism, while SnPP increased it (Figure 3A). We also infected thioglycollate-elicited macrophages in vitro and treated them with CoPP or SnPP. Treat-

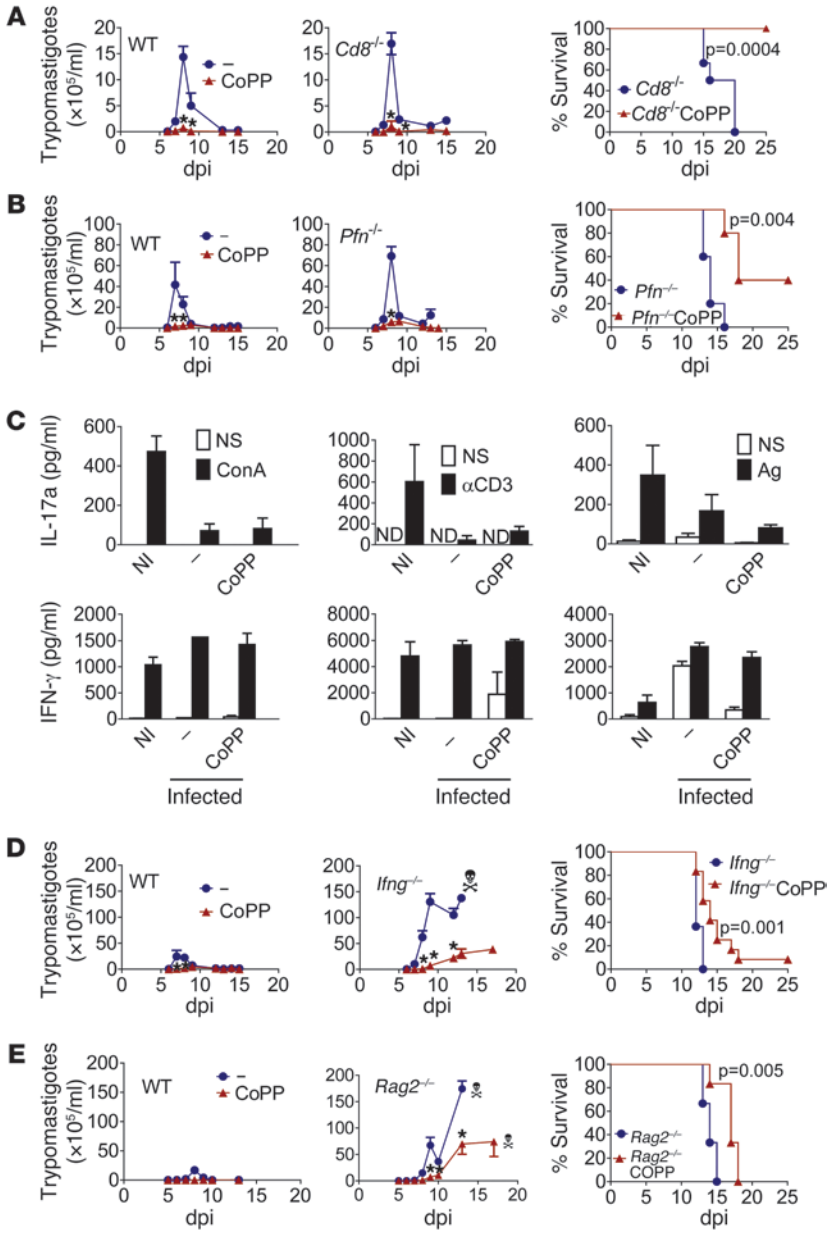

Figure 2
CoPP-mediated reduction of *T. cruzi* parasitemia does not involve adaptive immunity. (**A**) Effect of CoPP or SnPP treatment on survival and mean parasitemia in wild-type control, *Cd8*$^{-/-}$ (n = 7–8), and (**B**) *Pfn*$^{-/-}$ mice (n = 6–9). (**C**) Cytokine production by splenocytes stimulated with ConA, anti-CD3 (for 24 hours), or *T. cruzi* antigen (Ag; for 48 hours). Splenocytes were pooled from 3–5 mice per group treated in vivo with CoPP at 9 dpi, and supernatants from 3 pools were analyzed by ELISA. (**D**) Effects of treatment with CoPP on survival and mean parasitemia of wild-type controls and *Ifng*$^{-/-}$ mice (n = 9–15 mice) or (**E**) *Rag2*$^{-/-}$ mice (n = 6). Experiments were performed twice, with similar results (**A**–**D**). ND, not detected; NI, noninfected; –, infected untreated controls. *P < 0.05 compared with infected nontreated controls. Error bars represent SEM.

ment with CoPP reduced macrophage parasitism, while SnPP increased it (Figure 3B). When trypomastigotes were allowed to mature, CoPP also reduced the numbers of trypomastigotes (Supplemental Figure 2A). Infected macrophages treated with CoPP had higher HO-1 expression (Supplemental Figure 2B). These data show that the HO-1 inducer CoPP reduces macrophage parasitism by *T. cruzi* in vivo and in vitro.

CoPP depends on macrophage physiology to reduce parasitism and does not act directly on the parasite. SnPP, CoPP, and the by-products of HO-1 activity biliverdin and bilirubin were unable to kill trypomastigotes in vitro, as determined by trypomastigote motility (Supplemental Figure 2C). In contrast to benznidazole, CoPP could not kill trypomastigotes even after 48 hours incubation, as assessed by propidium iodide (PI) staining (Supplemental Figure 2D). Neither the supernatant of macrophages incubated with CoPP nor the sera from mice treated with CoPP were able to kill trypomastigotes in vitro, indicating that no trypanocidal soluble factor is induced in response to CoPP (Supplemental Figure 2, E–G). However, treatment of macrophages with CoPP after differentiation of trypomastigotes into amastigotes (24 hours) did reduce infection (Supplemental Figure 2H). Likewise, CoPP administered to mice starting at 2 dpi (allowing differentiation into amastigotes) also reduced parasitemia (Supplemental Figure 2I), indicating that CoPP does not target amastigogenesis. However, CoPP did not alter parasite burden in the fibroblastic cell line L929 (Figure 3C), indicating that its effects depend on macrophage physiology rather than acting directly on the parasite.

HO-1 overexpression reduces macrophage parasitism, but CoPP activates redundant mechanisms of T. cruzi elimination through Nrf2 activation. CoPP is known to decrease NRF2 degradation, thereby increasing expression of HO-1 (28). We tested whether HO-1 overexpression could mimic the decrease in parasitism mediated by CoPP in THP-1 cells (Figure 3D). Transfection of THP-1 cells with an *Hmox1* vector markedly decreased parasitism as compared with mock-transfected controls (Figure 3D). We then tested whether CoPP required HO-1 expression in order to reduce parasitism. CoPP similarly decreased the parasitism of bone marrow macrophages (BMMs) from wild-type and HO-1–deficient (*Hmox1*$^{-/-}$) mice (Figure 3E). These results suggest that other NRF2 target genes induced by CoPP can replace HO-1 in its absence to reduce parasitism. Indeed, CoPP failed to reduce parasitism in *Nrf2*$^{-/-}$ BMMs (Figure 3F), demonstrating that NRF2 is required for CoPP to reduce parasitism. THP-1 cells transfected with *Nrf2* showed reduced parasitism compared with mock-transfected controls (Figure 3G). We also incubated infected macrophages with the NRF2 activators oltipraz, sulforaphane, pterostilbene, and resveratrol. Similar to CoPP (Figure 3H), the other NRF2 activators reduced macrophage parasitism in a dose-dependent fashion (Figure 3, I–L). Resveratrol and pterostilbene administration in vivo also reduced parasitemia (Figure 3M). Together, our data indicate that genes activated by NRF2 redundantly control resistance to *T. cruzi* infection in macrophages.

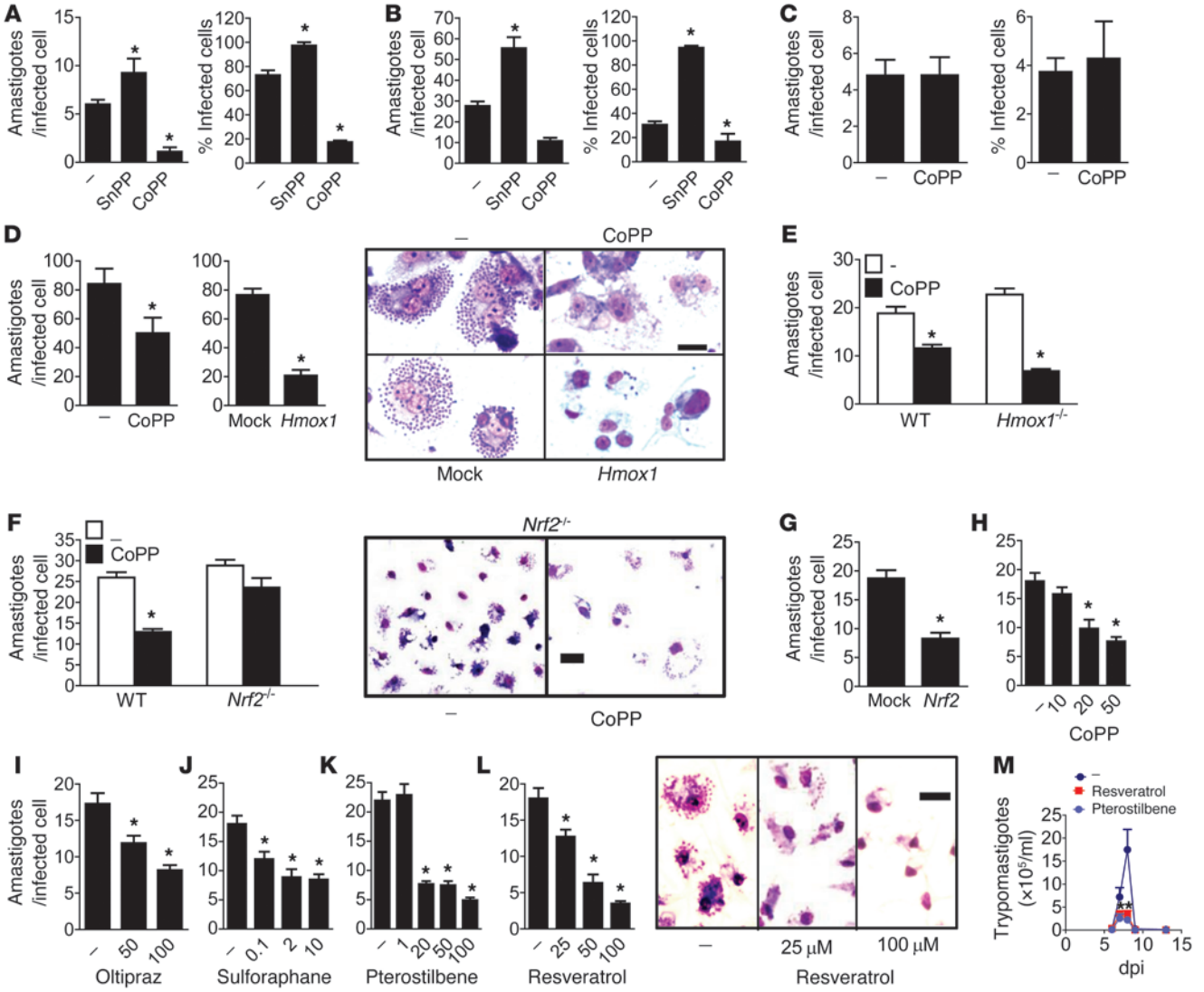

Figure 3

CoPP reduces parasitism via macrophage physiology and NRF2 target genes. (**A**) Effects of in vivo treatment with CoPP or SnPP on the mean parasite burden of peritoneal macrophages at 8 dpi ($n = 3$ mice/group). Peritoneal cells were cultured for an additional 48 hours before cells were fixed. (**B**) Effects of treatment with CoPP or SnPP on the mean parasite burden of thioglycollate-elicited macrophages infected in vitro. (**C**) Effects of treatment with CoPP on the mean parasite burden of L929 fibroblast cells. (**D**) Effects of prior transfection of THP-1 cells with HO-1 or empty vector on mean parasite burden. (**E**) Effects of treatment with CoPP on mean parasite burden of BMMs derived from wild-type and *Hmox1*$^{-/-}$ mice or (**F**) *Nrf2*$^{-/-}$ mice. (**G**) Effects of prior transfection of THP-1 cells with *Nrf2* or empty vector on mean parasite burden. (**H**–**L**) Dose-dependent decreases in macrophage parasitism with the NRF2 activators. (**M**) Mean parasitemia during acute infection ($n = 8$) in mice treated with pterostilbene or resveratrol. Thioglycollate-elicited macrophages were infected with 3:1 trypomastigotes in vitro for 12 hours and treated with drugs for 48 hours. Each experiment was performed with 2 independent samples of cells, and results for 1 sample are shown. Cells were stained with Giemsa, and amastigotes were counted in each of 100 infected cells. The mean percentage of infected cells was calculated for each field, and 20 fields were assessed. All experiments were performed at least twice, with similar results. *$P < 0.05$ compared with infected nontreated controls. Error bars represent SEM. Scale bars: 20 μm.

Apoptosis, NO, TNF, and type I IFN are not involved in the protective effect of CoPP in T. cruzi infection. As our results indicated that CoPP targeted macrophage physiology to reduce parasite burden, we tested whether CoPP relied on classical mechanisms of parasite elimination by macrophages. Apoptosis is a common response to intracellular infections that reduces infection reservoirs. We investigated whether the effect of CoPP on parasite burden was due to the increased survival of uninfected cells. We found that treatment with CoPP reduced apoptosis of all cells following exposure to *T. cruzi*, irrespective of the whether the cells were infected (Figure 4B).

Production of type I IFN by infected cells represents a mechanism of defense against *T. cruzi* (34). As HO-1 expression in macrophages is required for IRF3 phosphorylation and IFN-β production in response to various stimuli (35), we tested whether treatment with CoPP would alter IFN-β production

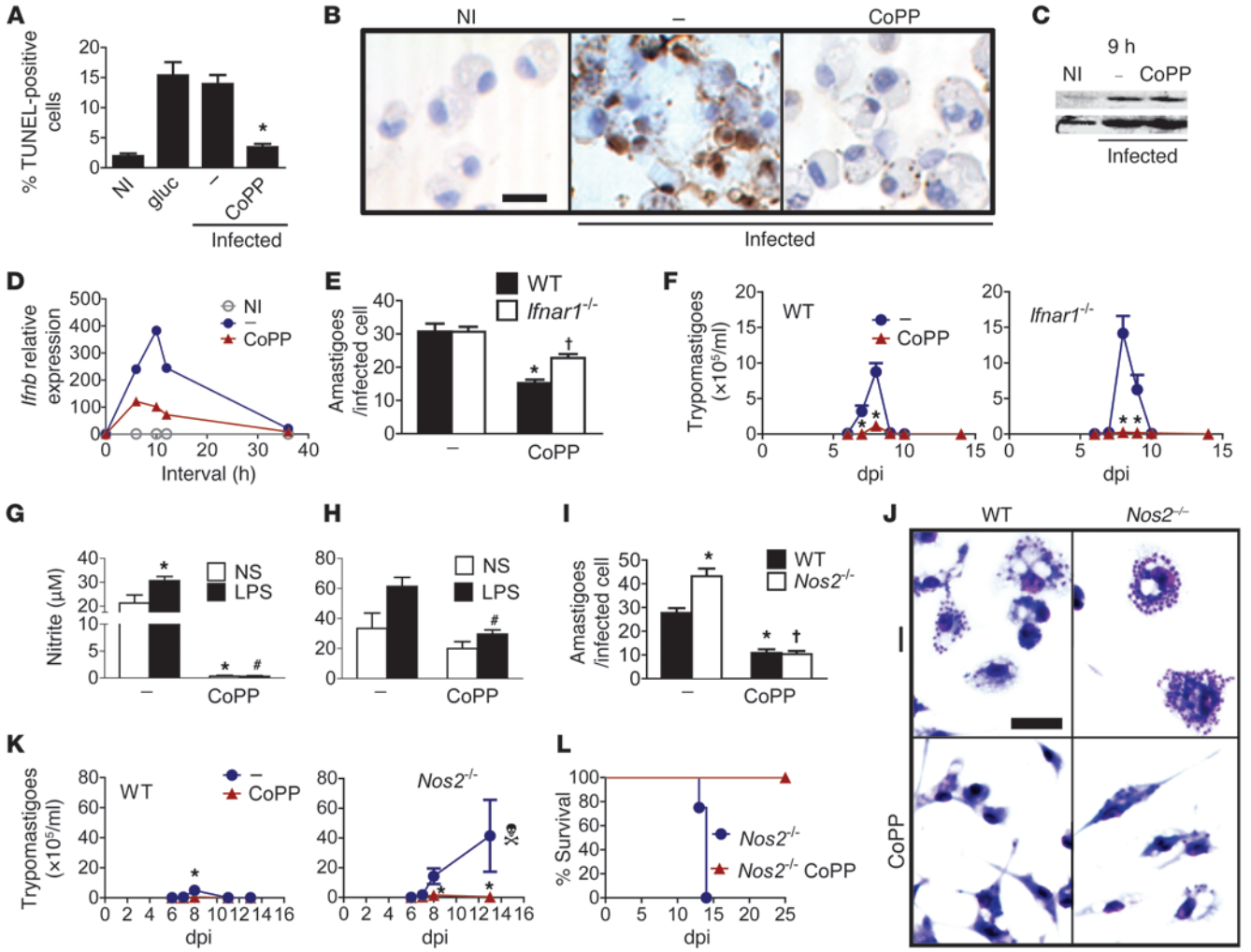

Figure 4

Classical mechanisms of parasite clearance are not responsible for the decreased parasitism mediated by CoPP. (**A**) Effects of CoPP on the mean percentage of TUNEL-positive cells (apoptotic) found in infected macrophages, as shown in **B**. Glucocorticoid-treated macrophages (gluc) are shown as a positive control. Amastigotes were also stained with TUNEL (33). Data represent percentages in 10–15 microscope fields (original magnification, ×40). Effects of CoPP on (**C**) IRF-3 phosphorylation in infected macrophages (immunoblots) and (**D**) the amounts of *IFN*-β transcripts (qRT-PCR). (**E**) Effects of CoPP on the mean parasite burden in infected macrophages derived from wild-type or *Ifnar1*$^{-/-}$ mice. (**F**) Effects of CoPP on the mean parasitemia of wild-type and *Ifnar1*$^{-/-}$ mice (n = 8 per group). (**G**) Effects of in vivo CoPP treatment on the mean nitrite production by LPS-stimulated peritoneal macrophages at 8 dpi. Cells were pooled from 3–5 mice/group, and results represent 3–4 pools (Griess). Effects of CoPP on infected macrophages: (**H**) Mean nitrite production upon LPS stimulation in vitro (results represent 3 independent samples evaluated by Griess); (**I**) Mean parasite burden of macrophages derived from wild-type or *Nos2*$^{-/-}$ mice (Giemsa), as shown in **J**. Effects of in vivo CoPP treatment on: (**K**) Mean parasitemia and (**L**) survival of wild-type and *Nos2*$^{-/-}$ mice (n = 4–6). Experiments were performed at least twice. Error bars represent SEM. $^{*}P < 0.05$ compared with infected untreated wild-type; $^{\#}P < 0.05$ compared with LPS-stimulated infected untreated macrophages; $^{\dagger}P < 0.05$ compared with infected untreated knockout mice. Scale bars: 20 μm.

during *T. cruzi* infection. Infection induced IRF3 phosphorylation in macrophages (36), but CoPP had no effect (Figure 4C). IFN-β production increased upon infection, but was attenuated in macrophages treated with CoPP (Figure 4D). CoPP reduced parasitism in macrophages from wild-type mice and to a lesser extent in macrophages from *Ifnar1*$^{-/-}$ mice (Figure 4E). However, treatment with CoPP reduced parasitemia of *Ifnar1*$^{-/-}$ (Figure 4F) mice to levels similar to those of wild-type mice.

Macrophages from CoPP-treated infected mice (8 dpi) produced less NO when stimulated with LPS ex vivo (Figure 4G). Macrophages infected in vitro and then treated with CoPP also produced less NO in response to LPS (Figure 4H). CoPP reduced parasitism in both wild-type and *Nos2*$^{-/-}$ (iNOS-deficient) macrophages (Figure 4, I and J). Treatment of *Nos2*$^{-/-}$ mice with CoPP reduced parasitemia and mortality (Figure 4, K and L). A similar profile was found for TNF (Supplemental Figure 3, A–E). These results demonstrate that conventional *T. cruzi* elimination mechanisms are not involved in the reduction of parasitism by CoPP.

Antioxidants decrease macrophage parasitism, while pro-oxidants promote T. cruzi growth and reverse the protective effects of CoPP. To confirm that infection promotes respiratory burst, we incubated noninfected and infected macrophages with the ROS probe

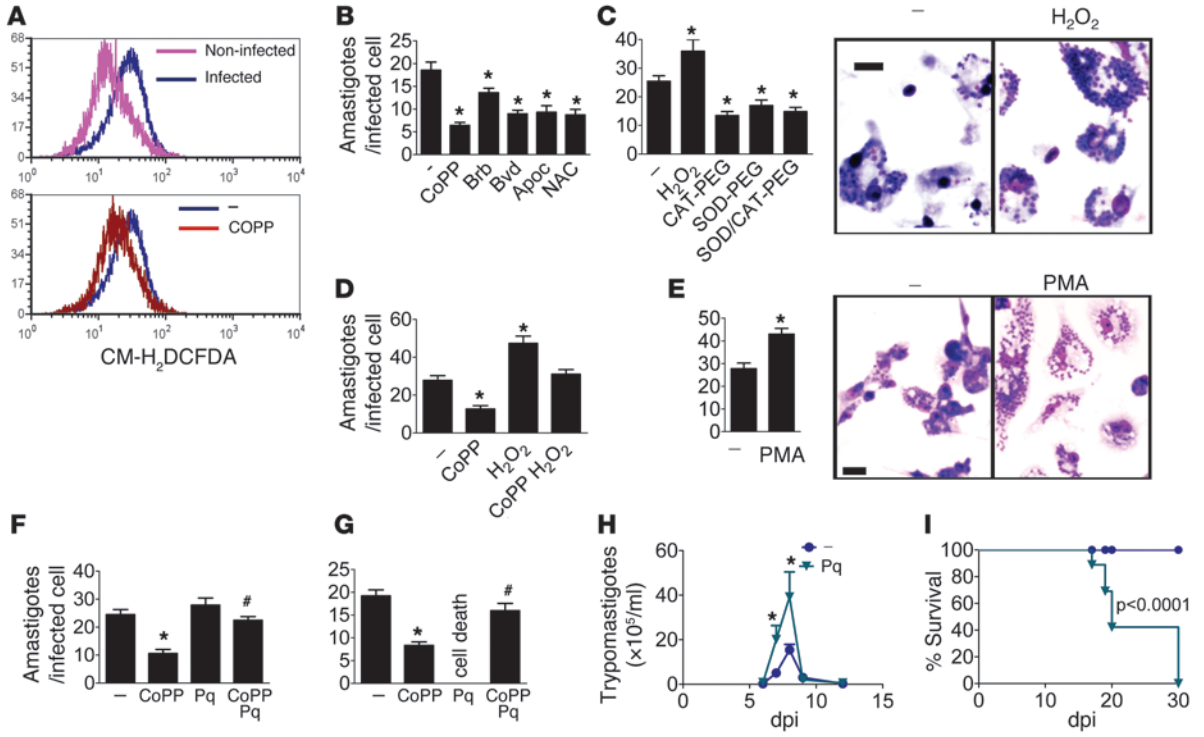

Figure 5
Oxidative stress promotes *T. cruzi* parasitism. (**A**) Flow cytometry quantification of ROS (CM-H_2DCFDA) in thioglycollate-elicited macrophages infected in vitro and left untreated (–) or treated with CoPP for 6 hours. (**B**) Parasite burden (Giemsa) in thioglycollate-elicited peritoneal macrophages infected in vitro and left untreated (–) or treated for 48 hours with CoPP, bilirubin (Bb), biliverdin (Bvd), apocynin (Apoc), or NAC; (**C**) H_2O_2, CAT-PEG, SOD-PEG, or SOD-PEG plus CAT-PEG; (**D**) CoPP, H_2O_2, or CoPP plus H_2O_2; (**E**) PMA; CoPP, paraquat (Pq; 10 μM [**F**] or 100 μM [**G**]), or CoPP plus paraquat. (**H**) Mean parasitemia and (**I**) survival of mice treated with paraquat ($n = 8$). Experiments were performed at least twice, with similar results. Error bars represent SEM. $^*P < 0.05$ compared with infected untreated controls. $^{\#}P < 0.05$ compared with CoPP-treated cells. Scale bars: 20 μm.

CM-H_2DCFDA. Infection increased fluorescence starting at 6 hours after infection (Figure 5A). As expected, CoPP partially prevented the increase in ROS induced by infection (Figure 5A). By 6 hours after treatment with CoPP, macrophage parasite burden was still similar among treated and nontreated cells (Supplemental Figure 4). The antioxidants superoxide dismutase–polyethylene glycol (SOD-PEG), catalase–polyethylene glycol (CAT-PEG), bilirubin, biliverdin, *N*-acetyl-cysteine (NAC), and apocynin all reduced parasitism (Figure 5, B and C). H_2O_2 alone promoted while coincubation with CoPP reversed the protective effects of CoPP (Figure 5D). Activation with PMA, which is known to promote respiratory burst, increased macrophage parasitism (Figure 5E). Low concentrations (10 μM) of the pro-oxidant paraquat did not promote parasitism but did reverse the protective effects of CoPP (Figure 5F). High concentrations (100 μM) promoted macrophage cell death, but CoPP plus paraquat prevented macrophage death and allowed parasitism (Figure 5G). Paraquat administration in vivo increased parasitemia and mortality of infected mice (Figure 5, H and I), indicating that this effect is also relevant in vivo. Infection of macrophages from mice deficient in NOX2 subunit *gp91^{phox}* resulted in reduced parasitism as compared with wild-type mice, and CoPP did not have a protective effect (Figure 6A). BMMs from *gp91$^{phox-/-}$* mice produced less ROS than cells from wild-type mice upon infection (Figure 6B). In fact, infected *gp91$^{phox-/-}$* mice also had reduced parasitemia (Figure 6C) and reduced parasite burden in their splenic macrophages as compared with wild-type mice (Figure 6D). Still, infected *gp91$^{phox-/-}$* mice treated with CoPP showed reduced parasitemia (Figure 6E), suggesting that CoPP also acts through non-NOX2-targeted mechanisms in vivo, though to a lesser extent. Nevertheless, infected *gp91$^{phox-/-}$* mice died late in acute infection (Figure 6F), while *gp91$^{phox-/-}$* mice treated with CoPP survived the acute infection. The cause of death of infected *gp91$^{phox-/-}$* mice and the mechanism of protection by CoPP remain to be investigated. Together, these results suggest that macrophage exposure to ROS promotes infection.

Cellular iron is mobilized by oxidative stress and fuels T. cruzi infection. Ferritin and ferroportin have antioxidant response element (ARE) sequence motifs in their promoters and are upregulated by NRF2 activators (37, 38). Ferritin-bound iron represents a redox-inert storage of iron. Intracellular microbes differ in the sources of iron they use, and although *Neisseria* scavenge iron-laden ferritin (39), the trypanosomatid *Leishmania donovani* feeds on only the labile iron pool (non-ferritin iron) (40). The sources of iron used by *T. cruzi* amastigotes as a nutrient are currently unknown. Reduction of the labile iron pool could potentially decrease the iron available for dividing amastigotes or, alternatively, reduce oxidative stress. Therefore, we tested whether reduction of labile iron pool could be responsible for the effects of CoPP.

Treatment with CoPP, as well as with the antioxidants NAC and apocynin, increased H-ferritin and ferroportin-1 (FPN1) expression in infected macrophages (Figure 7A). Increased expression of H-ferritin and FPN1 is known to reduce the labile iron pool

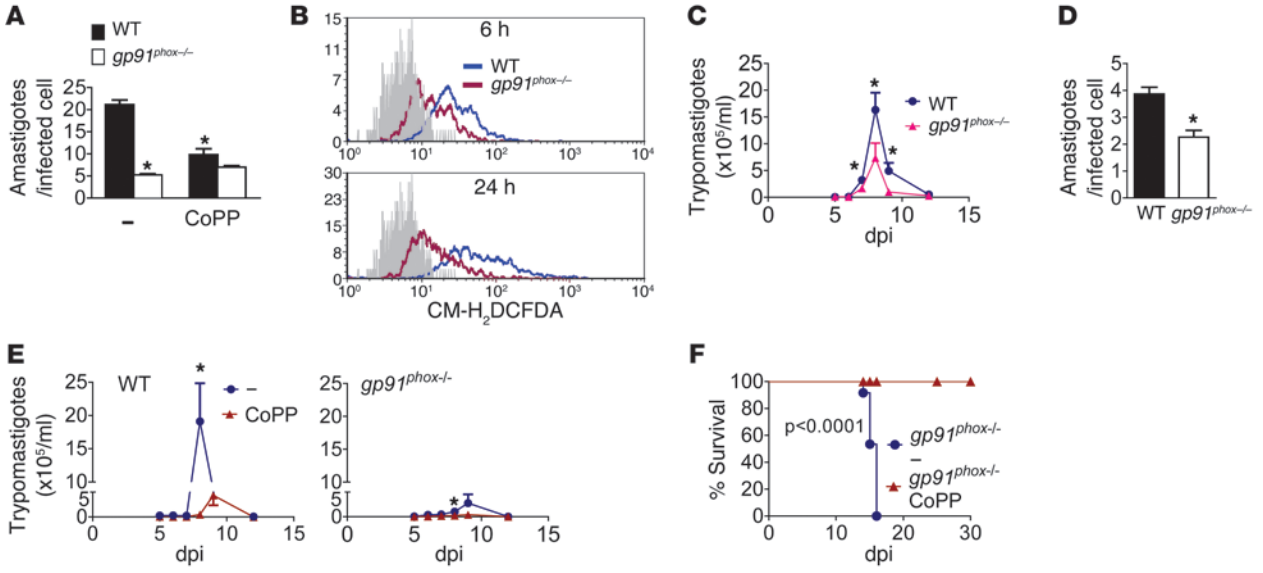

Figure 6
Effects of *gp91phox* on *T. cruzi* infection. (**A**) Effects of CoPP on the parasite burden of in vitro infected macrophages derived from wild-type or *gp91phox–/–* mice (Giemsa). (**B**) Flow cytometry quantification of ROS (CM-H_2DCFDA probe) in BMMs from wild-type or *gp91phox–/–* mice after infection. Non-labeled controls are shown in gray. (**C**) Mean parasitemia of wild-type and *gp91phox–/–* mice (n = 7). (**D**) Parasite burden in peritoneal macrophages taken from wild-type and *gp91phox–/–* mice at 8 dpi. Cells were cultured for an additional 48 hours before they were fixed and stained. The graphs show the mean ± SEM of the parasite burden in each individual mouse (n = 4 mice/group). (**E**) Mean parasitemia (n = 5) and (**F**) survival of wild-type and *gp91phox–/–* mice left untreated (n = 12) or treated with CoPP (n = 5). Error bars represent SEM. *P < 0.05 compared with infected untreated controls.

(41). Using the quenching of calcein fluorescence as an indicator of free iron, we measured the labile iron pool by flow cytometry. Treatment of infected macrophages with the antioxidants CoPP, NAC, and apocynin increased calcein fluorescence compared with infected untreated cells (Figure 7B), indicating a reduction in the labile iron pool. Concomitant treatment with antioxidants and Fe^{2+} reversed the increase in calcein fluorescence.

Transfection of THP-1 cells with H-ferritin as well as incubation with apoferritin reduced parasitism (Figure 7, C and D). The iron chelator desferrioxamine (DFO), which decreases intracellular iron availability, also reduced macrophage parasitism (Figure 7E). BMP and IL-6 promote degradation of FPN1 through hepcidin induction and have similar autocrine effects on macrophages (42–44). Treatment with IL-6 or Fe^{2+} did not alter parasitism, but incubation with both simultaneously, which is known to induce iron loading, increased parasitism (Figure 7F). Dorsomorphin, an inhibitor of the BMP/Smad4 pathway that ultimately promotes ferroportin expression (45), reduced macrophage parasitism, and Fe^{2+} reversed this effect (Figure 7G). Incubation with Fe^{2+} also reversed the CoPP-mediated decrease in parasitism, as well as that produced by NAC or apocynin (Figure 7, H–J). Fe^{2+} also enhanced parasitism in macrophages from *gp91phox–/–* mice (Figure 7K). Together, these results indicate that increases in the labile iron pool are associated with increased macrophage parasitism.

As HO-1 is known to affect iron physiologically in vivo (46, 47), we determined whether peroral iron was capable of attenuating the effects of CoPP. Administration of $FeSO_4$ increased parasitemia (Figure 7L). When given with CoPP, peroral $FeSO_4$ reversed the CoPP-mediated decrease in parasitemia, resulting in levels of parasitemia similar to those of mice treated with $FeSO_4$ (9 dpi) only. Mortality followed a similar pattern (Figure 7M). These results suggest that CoPP-mediated reduction of the labile iron pool is involved in reducing parasite burden.

Discussion

To date, little is known about the role of ROS in *T. cruzi* parasite burden. In macrophages with an exhausted respiratory burst, *T. cruzi* growth increased, suggesting that ROS are protective (48). This finding was further supported by the association between macrophage trypanocidal activity and the production of hydrogen peroxide (49). Others have not found evidence that macrophage-derived ROS contribute to *T. cruzi* killing (50, 51). However, previous studies have shown that amastigote burden significantly decreased when preinfected macrophages were treated with SOD and catalase during stimulation with IFN-γ (52). The authors interpreted this finding as a consequence of the increased NO production, but no functional studies supported this conclusion. Recently, evidence for peroxynitrite as a mediator of *T. cruzi* killing was found in IFN-γ/LPS–preactivated macrophages (10), but the subject was not approached systematically in unstimulated macrophages. To our knowledge, we have performed the first systematic study of *T. cruzi* infection under pro- or antioxidant conditions. This study indicates that ROS contribute to Y strain amastigote growth inside macrophages and increase overall parasitism.

Our results consistently point to oxidative stress as an enhancer of *T. cruzi* infection in macrophages. Indeed, the reduced macrophage parasitism in apocynin (NOX2 inhibitor)–treated and *gp91phox–/–* macrophages indicate that ROS generated during respiratory burst are counterproductive against *T. cruzi* infection. This finding is corroborated by the observation that

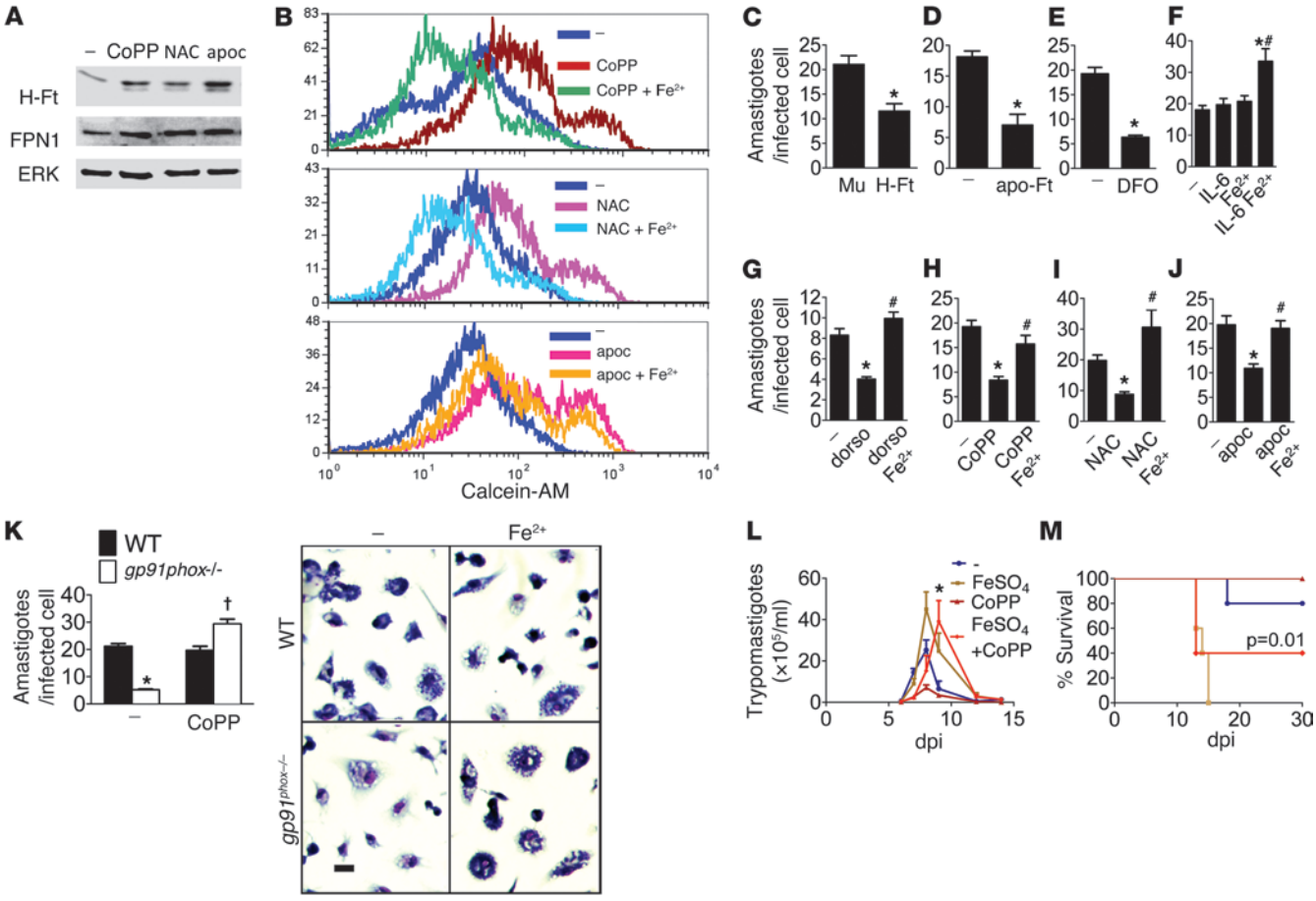

Figure 7

Cellular iron is mobilized by oxidative stress and fuels *T. cruzi* infection. (**A**) Antioxidants increase H-ferritin (H-Ft) and FPN1 expression (immunoblot). Extracts were prepared from infected thioglycollate-elicited peritoneal macrophages treated for 12 hours with CoPP, NAC, or apocynin. (**B**) Antioxidants reduce the labile iron pool. The quenching of calcein fluorescence was measured by flow cytometry as an indicator of labile iron. Thioglycollate-elicited peritoneal macrophages were infected in vitro and left untreated (–) or treated for 6 hours with antioxidants (CoPP, NAC, apocynin) with or without Fe^{2+}. (**C**) Parasite burden in THP-1 cells transfected with H-ferritin or mutant nonfunctional ferritin (Mu) 48 hours after infection. Parasite burden in thioglycollate-elicited peritoneal macrophages infected in vitro and left untreated (–) or treated with (**D**) apo-ferritin (apo-Ft); (**E**) DFO; Fe_2SO_4 alone or (**F**) added to IL-6, (**G**) dorsomorphin (dorso), (**H**) CoPP, (**I**) NAC, or (**J**) apocynin for 48 hours. (**K**) Parasite burden in thioglycollate-elicited peritoneal macrophages taken from wild-type or *gp91*$^{phox-/-}$ mice infected in vitro and treated with Fe_2SO_4 for 48 hours. Effects of treatment with CoPP and Fe_2SO_4 on (**L**) mean parasitemia and (**M**) survival of mice (n = 8–10). Error bars represent SEM. In **C**–**K**, cells were stained with Giemsa, and amastigotes were counted in each of 100 infected cells and expressed as mean ± SEM. Experiments were performed at least twice. *P < 0.05 compared with infected untreated wild-type controls; $^{\#}P$ < 0.05 compared with IL-6– (**F**), dorsomorphin- (**G**), CoPP- (**H**), NAC- (**I**), or apocynin-treated cells (**J**); $^{\dagger}P$ < 0.05 compared with infected knockout mice. Scale bars: 20 μm.

PMA and H_2O_2 increase parasitism. We also observed reduced parasitemia and reduced macrophage parasitism in infected *gp91*$^{phox-/-}$ mice. These data are in contrast with the reported increased parasite burden in apocynin-treated mice infected with strain Sylvio X10/4 at 35 dpi (53). However, these authors did not evaluate macrophage parasitism in their study. It is possible that ROS generation by NOX2 is required to control infection in particular tissues, to establish a late adaptive response, or to combat particular *T. cruzi* strains.

Evidence that oxidative stress fuels infection also comes from the observation that mice treated with the pro-oxidant paraquat had increased parasitemia, while mice treated with the NRF2 activators resveratrol and pterostilbene or deficient in *gp91*^{phox} expression had decreased parasitemia. Others have previously reported that treatment with NAC reduced *T. cruzi* parasitemia (54) and also parasite burden in *Leishmania* infection (55), which resisted oxidative stress (56).

Although transfection with HO-1 mimicked treatment with CoPP and reduced parasite burden, NRF2 target genes (other than HO-1) probably replaced HO-1 in its absence, as CoPP reduced parasite burden in macrophages from *Hmox1*$^{-/-}$ mice but not *Nrf2*$^{-/-}$ mice. These data demonstrate that CoPP operates through NRF2 target genes to reduce parasitism and were also corroborated by the ability of other reputed NRF2 activators to reduce macrophage parasitism and parasitemia.

Treatment with SnPP, an inhibitor of HO-1 activity, increased macrophage parasitism, but BMMs from *Hmox1*$^{-/-}$ and *Nrf2*$^{-/-}$ mice had parasitism similar to that in wild-type mice. It is possible

that HO-1 controls infection and that the sudden loss of its activity increases parasite burden. In this case, compensatory mechanisms of parasite control could explain why *Hmox1*$^{-/-}$ and *Nrf2*$^{-/-}$ macrophages did not show increased parasite burden.

As we found that treatment with CoPP prevents apoptosis in *T. cruzi*–infected macrophages, it could be argued that CoPP acts by leaving macrophages intact to fight infection. However, macrophages can withstand heavy infection before rupturing, so survival alone does not explain how the macrophages eliminate the parasite (33). We showed here that CoPP reduces parasitism despite severely reducing NO, a classical mechanism by which macrophages eliminate *T. cruzi*. These data indicate that CoPP triggers a rather unconventional mechanism of *T. cruzi* elimination. It is nevertheless possible that other cell types have mechanisms distinct from those of macrophages to fight infection and can benefit from the lower rate of apoptosis mediated by CoPP.

T. cruzi amastigotes require iron to grow in axenic cultures (57). Chelating iron reduces *T. cruzi* infection in macrophages (58) and mice (59), while iron-rich diets or iron-dextran worsen infection (60), suggesting that iron is critical for *T. cruzi* growth. Here, we found that several strategies to increase the labile iron pool resulted in increased parasitism, while incubation of infected macrophages with Fe^{2+} reversed the decrease in parasitism mediated by CoPP and other antioxidants. In vivo, peroral $FeSO_4$ also reversed the reduction in parasitemia mediated by CoPP. These results indicate that antioxidants act by precluding iron uptake by the parasite or by reversing the oxidative stress generated by Fe^{2+}, which would then increase parasitism through unknown mechanisms. Indeed, treatment with antioxidants increased expression of H-ferritin and FPN1 and increased the fluorescence of calcein, demonstrating that antioxidants reduce the labile iron pool during infection. These data also suggest that the decrease in the labile iron pool is involved in preventing macrophage parasitism.

Extensive literature describes HO-1 as an anti-immunogenic, antiinflammatory, and antioxidant enzyme (13). ROS production is a well-known mechanism of pathogen elimination through respiratory burst in macrophages. Though it was expected that induction of HO-1 in infections would cripple the defenses and allow pathogen growth, we observed the exact opposite during *T. cruzi* infection. In fact, a number of recent findings point to NRF2 and HO-1 as mediators of innate immunity. Pathogen burden has been shown to be decreased by HO-1 overexpression in hepatitis C–infected hepatocytes (61, 62), hepatitis B–infected mice (21), enterovirus 71 infection in neuroblastoma (17), and HIV-infected monocytes (23); however, the mechanism of this is unknown. The HO-1–mediated increase in bacterial clearance during sepsis has been associated with increased phagocytosis that could potentially mediate the protective effects (25). Antioxidants have been found to reduce pathogen burden in a number of infections (16–18), while hydrogen peroxide increased *Mycobacterium abscessus* burden (19), indicating that ROS can be counterproductive in some infections. We showed here that HO-1 induction reduces macrophage parasitism and parasitemia, which correlated positively with oxidative stress and the labile iron pool. Whether this is the main mechanism by which NRF2 target genes operate to control infections remains to be determined.

In conclusion, we showed that *T. cruzi* parasitism correlated with oxidative stress, while CoPP reduced *T. cruzi*-induced ROS production and infection in an NRF2/HO-1–dependent manner. Similar to our findings, melatonin, a hormone that activates antioxidant mechanisms through NRF2 activation (63), has been shown to decrease parasitemia and mortality (64). Also, 15d-PGJ2, an agonist of PPARγ that induces NRF2/HO-1 expression in macrophages (65), decreases *T. cruzi* parasitism (66), as does curcumin (67), a reputed NRF2 activator. It remains to be elucidated whether melatonin, 15d-PGJ2, and curcumin act through NRF2/HO-1–dependent mechanisms to reduce *T. cruzi* infection. The exact mechanism by which oxidative stress enhances *T. cruzi* infection remains to be clarified, though iron mobilization is a possibility. We believe the association between NRF2/HO-1 induction and protection against *T. cruzi* parasite burden and tissue damage demonstrated here opens a new avenue for the development of drugs against this pathogen.

Methods

Parasites, mice, in vivo infection, and treatments. *T. cruzi* Y strain trypomastigotes were maintained by blood passage in mice every 7 days. Trypomastigotes were isolated from heparinized blood by low-speed centrifugation and collection of the parasites that swam out of the pellet. Experimental infection was performed by i.p. injection of 10^4 blood trypomastigotes. In vitro experiments were performed with Y strain trypomastigotes obtained from infected LLCKM2 cell cultures (grown in 10% FCS supplemented DMEM). Parasitemia was evaluated in tail blood. C57BL/6 mice were bred and maintained in our facilities (UFRJ, IMPPG). *gp91*$^{phox-/-}$ (C57BL/6) mice were provided by Leda Q. Vieira (Universidade Federal de Minas Gerais [UFMG], Belo Horizonte, Brazil) and José Carlos Alves Filho (Universidade de São Paulo [USP], Ribeirão Preto, Brazil). *Hmox1*$^{-/-}$ (BALB/c) (68) and *Nrf2*$^{-/-}$ (C57BL/6) (69) bone marrow samples were a gift from Miguel Soares (Instituto Gulbenkian de Ciência, Oleiras, Portugal), and its use was authorized by Mark Perrela and RIKEN BRC through the National Bio-Resource Project of the Ministry of Education, Culture, Sports, Science and Technology (MEXT), Japan, respectively. *Nos2*$^{-/-}$, *Tnfr1*$^{-/-}$, *Cd8*$^{-/-}$, and *Pfn*$^{-/-}$ mice (all on the C57BL/6 background) were obtained from Centro de Criação de Animais de Laboratório (Cecal, Fiocruz, Rio de Janeiro, Brazil). *Ifnar1*$^{-/-}$ (129Sv) and wild-type mice were obtained from USP. *Ifng*$^{-/-}$ (C57BL/6) mice were obtained from both Cecal and Instituto Nacional del Cáncer (INCA, Rio de Janeiro, Brazil). CoPP, SnPP, biliverdin hydrochloride (Blv), and bilirubin were purchased from Frontier Scientific, dissolved in 0.2 M NaOH, neutralized to pH 7.2 with 1 M HCl, and adjusted to the desired concentrations with PBS. Treatments were performed by daily i.p. injection of vehicle or 5 mg/kg SnPP or CoPP. Treatment with CoPP or SnPP started on day 1 or 2 hours after infection, with similar results, except in Supplemental Figure 2J, where CoPP was started at 2 dpi. Prolonged treatment with CoPP (but not with SnPP) resulted in high mortality of mice in control experiments; therefore, we stopped treatment after the peak of parasitemia (8–10 dpi). Treatment with peroral $FeSO_4$ was performed by gavage (40 mg/kg) from 0 to 9 dpi. Paraquat was diluted in PBS (5 mg/kg) and injected i.p. in mice daily from 0 to 8 dpi. Resveratrol (3 mg/kg) and pterostilbene (2 mg/kg) were administered i.p. from 0 to 9 dpi (diluted in pure ethanol and then in PBS).

Parasite burden in macrophages from infected mice. Peritoneal cells from mice infected and left untreated or treated with apocynin, CoPP, or SnPP were collected at 8 dpi and seeded on coverslips inside 24-well plates for 48 hours in complete RPMI. Coverslips were then processed as described for in vitro assays of parasite burden.

In vitro assays for parasite burden. Thioglycollate-elicited peritoneal macrophages, BMMs, THP-1 differentiated macrophages, or L929 fibroblasts were used in these assays. THP-1 cells were differentiated as described below. Thioglycollate (4%) was injected i.p. into C57BL/6 mice, and peritoneal cells were collected by chilled RPMI washes 4 days after injection

to obtain elicited macrophages. BMMs were obtained by differentiation in vitro. Femurs and tibiae were cut at the ends and flushed with RPMI medium. Bone marrow cells were seeded at 4×10^6/ml per 100-mm^2 dish in 10 ml complete medium (RPMI [Gibco, Invitrogen] supplemented with 20% inactivated FCS, L-glutamine, HEPES, β-mercaptoethanol, and penicillin/streptomycin) with 20% conditioned medium (containing M-CSF, isolated from L929 cell cultures) for 4 days. Then, fresh medium was added, and cells were cultured until day 7. Cells were then harvested and used to seed round glass coverslips. A sample containing 3×10^5 to 5×10^5 elicited macrophages or BMMs was used to seed glass coverslips and left to adhere for 2 hours and rest for 24 hours. A sample containing 10^5 L929 fibroblasts was used to seed glass coverslips for 2 hours. Non-adherent cells were washed away before infection. Trypomastigotes obtained from cultures (as described above) were used to infect cells at a 3:1 (macrophages) or 10:1 (L929 cells) ratio for 12 hours, and then cultures were washed in RPMI. Drugs were diluted in complete RPMI and added to infected cultures for 48 hours. Then, cells were washed, fixed in absolute methanol, and stained with Giemsa (Sigma-Aldrich). Cells were then cleared and dehydrated in a xylol-acetone gradient, and slides were mounted with Entellan and photographed under an Olympus microscope (CX21, ×400 magnification). Pictures were printed, and amastigotes were identified and counted in samples of 40–200 infected macrophages from each group. Percentages of infected cells were determined from 20 pictures per group. In general, the percentage of infected cells paralleled amastigote burden within 48 hours, so we used amastigote burden to indicate parasitism. The following drugs were used in these assays: CoPP (50 μM, as determined by the dose-response curve in Figure 3), SnPP (50 μM), biliverdin (50 μM), and bilirubin (10 μM) (Frontier Scientific); resveratrol, pterostilbene, sulforaphane, and oltipraz (as determined by dose-response; Sigma-Aldrich); dorsomorphin (compound C, 10 μM, Sigma-Aldrich); mIL-6 (50 ng/ml, PeproTech); apocynin (1 mM; Sigma-Aldrich); NAC (10 μM, Sigma-Aldrich); $FeCl_3$ (100 μM, Sigma-Aldrich); $FeSO_4$ (100 μM, Sigma-Aldrich); DFO mesylate (DFO, 50 μM, Sigma-Aldrich); H_2O_2 (100 μM; 200 μM to reverse CoPP effects); PMA (200 ng/ml, Sigma-Aldrich); SOD-PEG (25 U/well); CAT-PEG (40 U/well); and paraquat (10–100 μM, Sigma-Aldrich).

Transfection of THP-1 cells with HO-1, NRF2, or H-ferritin. THP-1 cells were plated on glass coverslips in 24-well dishes (300,000 cells/dish) and differentiated into macrophages with PMA (40 ng/ml) for 72 hours, and then cultured for an additional 24 hours in DMEM supplemented with 10% fetal bovine serum in a 5% CO_2 humidified atmosphere. The cells were transiently transfected with 800 ng of pcDNA 3.1 HO.1 or empty pcDNA 3.1 (Invitrogen) plasmids using Lipofectamine 2000 (Invitrogen). The levels of HO-1 expressed were measured by Western blotting 24 hours after transfections. Similar procedures were performed with 800 ng of pcDNA 3.1 NRF2 or empty pcDNA 3.1 (Invitrogen), ferritin pSG5 WT, and ferritin 222 pShuttleCMV (mutant ferritin) before differentiation with PMA.

Parasite burden in macrophages from infected mice. Peritoneal cells from infected mice treated with vehicle, apocynin, CoPP, or SnPP were collected at 8 dpi and seeded on coverslips inside 24-well plates for 48 hours in complete RPMI. Coverslips were then processed as described for in vitro assays of parasite burden.

Trypomastigote viability. Trypomastigotes (5×10^5 to 5×10^6) were treated in 96-well plates (as described for in vitro macrophage studies), and motility was monitored as an indicator of viability after 24–48 hours.

TUNEL assay for apoptosis. Thioglycollate-elicited peritoneal macrophages were cultivated in 24-well plates (10^6/well), infected with trypomastigotes (3:1) for 12 hours, then washed and treated for 48 hours. Macrophages were then removed from plates by trypsinization and subjected to TUNEL staining (ApoTag Plus Peroxidase in Situ Apoptosis Kit, Millipore) according to the manufacturer's instructions.

Flow cytometry. Thioglycollate-elicited peritoneal macrophages were collected as described above, resuspended in RPMI, left to adhere in 48-well plates for 4 hours, and then washed and infected with 10:1 trypomastigotes for 1 hour in complete RPMI. Cells were again washed and reincubated with complete RPMI with the indicated drug for 6 hours, and then washed and removed from plates using a rubber policeman. Macrophages were incubated for 45 minutes with CM-H_2DCFDA (Invitrogen) under 5% CO_2 atmosphere; data were acquired with a flow cytometer (FACScan, BD). In calcein studies, thioglycollate-elicited peritoneal macrophages were left to adhere in 48-well plates for 24 hours and then washed and infected with 3:1 trypomastigotes for 12 hours in complete RPMI. Macrophages were then washed and loaded with the iron-sensitive fluorophore calcein-AM (Sigma-Aldrich) by preexposing the cells to 2 μM calcein-AM in iron-free PBS (Gibco, Invitrogen) for 15 minutes at 37°C under 5% CO_2 atmosphere. Then, cells were scraped off the plate with a rubber policeman, and data were acquired with a flow cytometer. In lymphocyte apoptosis studies, spleen cell suspensions were prepared, and red blood cells were lysed with ACK buffer. Lymphocytes were then washed and plated in U-bottomed 96-well plates at a density of 10^6/100 μl, pelleted, and double-labeled with appropriate antibodies (CD4-PE; CD8-PE; CD69-FITC; all from BD Biosciences — Pharmingen) in labeling buffer (PBS with 5% FCS, 5% normal rabbit serum, 0.5% BSA, and 0.5% NaN_3). For apoptosis studies, cells were then washed, resuspended in annexin V buffer (BD Biosciences — Pharmingen), and analyzed in a flow cytometer.

Cytokine production by splenocytes. Spleen cell suspensions (10^6/100 μl) from uninfected, infected control, and infected CoPP/SnPP-treated mice were prepared at 9 dpi. Cells were seeded in 96-well U-bottomed plates and stimulated for 24 hours with ConA (Sigma-Aldrich, 5 μg/ml), plate-bound anti-CD3 (prepared by incubating 1 mg/ml 2C11 antibody from BD Biosciences — Pharmingen in PBS for 12 hours and then washing) or for 48 hours with *T. cruzi* antigen (prepared by 10 freeze-and-thaw cycles applied to 10^8 culture trypomastigote pellets; a 5×10^6 parasite equivalent was used per well). Supernatants were frozen until detection of IL-4, IL-17A, or IFN-γ by ELISA (PeproTech).

NO and TNF production by macrophages. Peritoneal macrophages from infected mice or thioglycollate-elicited macrophages infected in vitro were used in these assays. Peritoneal washes from infected untreated or drug-treated mice were harvested at 8 dpi (Figure 4A) or 3 dpi (data not shown; similar results). Cells were left to adhere for 4 hours, then incubated with LPS (100 ng/ml LPS 011B4 from *E. coli*, InvivoGen) for 24 or 48 hours. Thioglycollate-elicited peritoneal macrophages (2×10^5) were diluted in RPMI, seeded in 96-well plates, and left to adhere for 2–4 hours. Non-adherent cells were washed away, and cells were allowed to rest in complete RPMI for 24 hours and then infected with trypomastigotes (3:1) for an additional 12 hours. Cells were washed and stimulated with LPS for 24 or 48 hours. Supernatants were assayed for NO (48 hours, Griess) or TNF (24 hours, ELISA, PeproTech).

Western blot for HO-1, IRF-3, H-ferritin, and FPN-1. Protein lysates from cultured cells were obtained with lysis buffer (50 mM Tris-HCl, pH 7.6, 150 mM NaCl, 1% NP-40, sodium deoxycholate 0.25%, 1 mM EDTA, 1 mM PMSF, 1 mM NaF) on ice for 10 minutes. Four-fold-concentrated SDS sample buffer was added to cell lysates (50 μg), which were boiled for 5 minutes, subjected to electrophoresis on a 8% SDS-polyacrylamide gel, and then transferred onto nitrocellulose. Protein molecular weight standards (Bio-Rad) were run concurrently. The nitrocellulose was blocked in TBS with Tween 20 (0.05%) containing 5% nonfat dry milk for 1 hour at room temperature. Blots were then probed overnight at 4°C with 1:2,000 monoclonal rabbit anti–HO-1, monoclonal goat anti–H-ferritin, monoclonal goat anti-FPN1 (Santa Cruz Biotechnology Inc.), or monoclonal mouse anti–p-IRF3 (Cell Signaling Technology). Bound primary antibody

was detected using donkey anti-goat, goat anti-rabbit, or anti-mouse IgG conjugated to horseradish peroxidase (Santa Cruz Biotechnology Inc.) diluted 1:1,0000, followed by incubation with the chemiluminescent substrate Luminol (Santa Cruz Biotechnology Inc.). The membrane was then exposed to X-ray film (Kodak). The same membrane was probed to detect the loading control protein ERK2 with mouse anti-ERK2 antibody (1:2,000, Santa Cruz Biotechnology Inc.).

Real-time qRT-PCR for IFN-β. Total RNA was extracted using TRIzol (Invitrogen), and 1 μg was reverse transcribed using M-MLV reverse transcriptase and random hexamer primers (Invitrogen). Subsequent real-time qRT-PCR analysis was performed on an ABI 7500 (Applied Biosystems) using SYBR green master mix (Applied Biosystems). Amplification conditions were as follows: 95°C (10 minutes), and 40 cycles of 95°C (15 seconds) and 60°C (60 seconds). All data were normalized to the corresponding HPRT expression, and the fold difference relative to the control level is shown. The analyses of relative gene expression data were performed with the $2^{-\Delta\Delta CT}$ method (70).

Histopathology. Hearts, quadriceps, and livers from infected mice were collected and preserved in formalin. Tissues were embedded in paraffin, cut in 5-μm sections, mounted on slides, and stained by a standard H&E technique. Sections were examined for parasite nests and photographed under an Olympus C21 microscope. Parasitism was expressed as either nests per 100 mm^2 (at 8 dpi, when parasites were confined to small nests) or number of parasites per field (at 15 dpi, ×400 magnification, parasites were counted on printed pictures, at least 20 per individual mouse slide).

Statistics. Statistical analysis was performed by Student's *t* test. The log-rank test was used to determine differences at the end point of the survival curves. Differences with a *P* value less than 0.05 were considered significant.

Study approval. The experiments were approved by the UFRJ Institutional Animal Welfare Committee (CEUA-CCS, protocol IMPPG-011).

Acknowledgments

This work was supported by CNPq, FAPERJ, Pronex, and Coordenação de Aperfeiçoamento de Pessoal de Nível Superior (CAPES). C.N. Paiva, R.T. Figueiredo, J. Lannes-Vieira, M.R. Fantappié, and M.T. Bozza received CNPq grants. We are indebted to Miguel Soares, Leo Otterbein, and Pedro Oliveira, who helped us with suggestions and reagents.

Received for publication December 2, 2011, and accepted in revised form April 18, 2012.

Address correspondence to: Claudia Neto Paiva or Marcelo Torres Bozza, Departamento de Imunologia, Instituto de Microbiologia, CCS Bloco D, UFRJ, Avenida Carlos Chagas Filho, 373 Cidade Universitária, Rio de Janeiro, RJ, 21941-902 Brazil. Phone: 55.21.22700990; Fax: 55.21.2560834; E-mail: cnpaiva@iname.com (C.N. Paiva), mtbozza@micro.ufrj.br (M. Torres Bozza).

Daniel F. Feijó's current address is: Departamento de Microbiologia Geral, Instituto de Microbiologia, Universidade Federal do Rio de Janeiro, Rio de Janeiro, Brazil.

1. Gupta S, Bhatia V, Wen JJ, Wu Y, Huang MH, Garg NJ. *Trypanosoma cruzi* infection disturbs mitochondrial membrane potential and ROS production rate in cardiomyocytes. *Free Radic Biol Med*. 2009;47(10):1414–1421.
2. Wen JJ, Garg N. Oxidative modification of mitochondrial respiratory complexes in response to the stress of *Trypanosoma cruzi* infection. *Free Radic Biol Med*. 2004;37(12):2072–2081.
3. Wen JJ, Vyatkina G, Garg N. Oxidative damage during chagasic cardiomyopathy development: role of mitochondrial oxidant release and inefficient antioxidant defense. *Free Radic Biol Med*. 2004;37(11):1821–1833.
4. Wen JJ, Bhatia V, Popov VL, Garg NJ. Phenyl-alpha-tert-butyl nitrone reverses mitochondrial decay in acute Chagas' disease. *Am J Pathol*. 2006;169(6):1953–1964.
5. McCord JM. Iron, free radicals, and oxidative injury. *J Nutr*. 2004;134(11):3171S–3172S.
6. Figueiredo RT, et al. Characterization of heme as activator of Toll-like receptor 4. *J Biol Chem*. 2007;282(28):20221–20229.
7. Fernandez PL, et al. Heme amplifies the innate immune response to microbial molecules through spleen tyrosine kinase (Syk)-dependent reactive oxygen species generation. *J Biol Chem*. 2010; 285(43):32844–32851.
8. Cardoni RL, Antunez MI, Morales C, Nantes IR. Release of reactive oxygen species by phagocytic cells in response to live parasites in mice infected with *Trypanosoma cruzi*. *Am J Trop Med Hyg*. 1997; 56(3):329–334.
9. Melo RC, Fabrino DL, D'Avila H, Teixeira HC, Ferreira AP. Production of hydrogen peroxide by peripheral blood monocytes and specific macrophages during experimental infection with *Trypanosoma cruzi* in vivo. *Cell Biol Int*. 2003;27(10):853–861.
10. Alvarez MN, Peluffo G, Piacenza L, Radi R. Intraphagosomal peroxynitrite as a macrophage-derived cytotoxin against internalized *Trypanosoma cruzi*: consequences for oxidative killing and role of microbial peroxiredoxins in infectivity. *J Biol Chem*. 2011;286(8):6627–6640.
11. Thomson L, Denicola A, Radi R. The trypanothione-thiol system in *Trypanosoma cruzi* as a key antioxidant mechanism against peroxynitrite-mediated cytotoxicity. *Arch Biochem Biophys*. 2003;412(1):55–64.
12. Zhang Q, Pi J, Woods CG, Andersen ME. A systems biology perspective on Nrf2-mediated antioxidant response. *Toxicol Appl Pharmacol*. 2010;244(1):84–97.
13. Gozzelino R, Jeney V, Soares MP. Mechanisms of cell protection by heme oxygenase-1. *Annu Rev Pharmacol Toxicol*. 2010;50:323–354.
14. Lin QS, Weis S, Yang G, Zhuang T, Abate A, Dennery PA. Catalytic inactive heme oxygenase-1 protein regulates its own expression in oxidative stress. *Free Radic Biol Med*. 2008;44(5):847–855.
15. Taille C, et al. Induction of heme oxygenase-1 inhibits NAD(P)H oxidase activity by down-regulating cytochrome b558 expression via the reduction of heme availability. *J Biol Chem*. 2004;279(27):28681–28688.
16. Fraternale A, et al. GSH and analogs in antiviral therapy. *Mol Aspects Med*. 2009;30(1–2):99–110.
17. Tung WH, Hsieh HL, Yang CM. Enterovirus 71 induces COX-2 expression via MAPKs, NF-kappaB, and AP-1 in SK-N-SH cells: role of PGE(2) in viral replication. *Cell Signal*. 2010;22(2):234–246.
18. Vlahos R, Stambas J, Bozinovski S, Broughton BR, Drummond GR, Selemidis S. Inhibition of nox2 oxidase activity ameliorates influenza a virus-induced lung inflammation. *PLoS Pathog*. 2011;7(2):e1001271.
19. Oberley-Deegan RE, et al. An oxidative environment promotes growth of *Mycobacterium abscessus*. *Free Radic Biol Med*. 2010;49(11):1666–1673.
20. Epiphanio S, et al. Heme oxygenase-1 is an anti-inflammatory host factor that promotes murine plasmodium liver infection. *Cell Host Microbe*. 2008;3(5):331–338.
21. Protzer U, et al. Antiviral activity and hepatoprotection by heme oxygenase-1 in hepatitis B virus infection. *Gastroenterology*. 2007;133(4):1156–1165.
22. Lehmann E, et al. The heme oxygenase 1 product biliverdin interferes with hepatitis C virus replication by increasing antiviral interferon response. *Hepatology*. 2010;51(2):398–404.
23. Devadas K, Dhawan S. Hemin activation ameliorates HIV-1 infection via heme oxygenase-1 induction. *J Immunol*. 2006;176(7):4252–4257.
24. Zaki MH, et al. Cytoprotective function of heme oxygenase 1 induced by a nitrated cyclic nucleotide formed during murine salmonellosis. *J Immunol*. 2009;182(6):3746–3756.
25. Chung SW, Liu X, Macias AA, Baron RM, Perrella MA. Heme oxygenase-1-derived carbon monoxide enhances the host defense response to microbial sepsis in mice. *J Clin Invest*. 2008;118(1):239–247.
26. Cho HY, et al. Antiviral activity of Nrf2 in a murine model of respiratory syncytial virus disease. *Am J Respir Crit Care Med*. 2009;179(2):138–150.
27. Reddy NM, et al. Innate immunity against bacterial infection following hyperoxia exposure is impaired in NRF2-deficient mice. *J Immunol*. 2009;183(7):4601–4608.
28. Shan Y, Lambrecht RW, Donohue SE, Bonkovsky HL. Role of Bach1 and Nrf2 in up-regulation of the heme oxygenase-1 gene by cobalt protoporphyrin. *FASEB J*. 2006;20(14):2651–2653.
29. Junqueira C, et al. The endless race between *Trypanosoma cruzi* and host immunity: lessons for and beyond Chagas disease. *Expert Rev Mol Med*. 2010;12:e29.
30. Padilla AM, Bustamante JM, Tarleton RL. CD8+ T cells in *Trypanosoma cruzi* infection. *Curr Opin Immunol*. 2009;21(4):385–390.
31. Bergeron M, Blanchette J, Rouleau P, Olivier M. Abnormal IFN-gamma-dependent immunoproteasome modulation by *Trypanosoma cruzi*-infected macrophages. *Parasite Immunol*. 2008;30(5):280–292.
32. Fraternale A, et al. The increase in intra-macrophage thiols induced by new pro-GSH molecules directs the Th1 skewing in ovalbumin immunized mice. *Vaccine*. 2010;28(48):7676–7682.
33. de Souza EM, et al. Host and parasite apoptosis following *Trypanosoma cruzi* infection in in vitro and in vivo models. *Cell Tissue Res*. 2003;314(2):223–235.
34. Costa VM, Torres KC, Mendonca RZ, Gresser I, Gollob KJ, Abrahamsohn IA. Type I IFNs stimulate nitric

oxide production and resistance to *Trypanosoma cruzi* infection. *J Immunol*. 2006;177(5):3193–3200.
35. Tzima S, Victoratos P, Kranidioti K, Alexiou M, Kollias G. Myeloid heme oxygenase-1 regulates innate immunity and autoimmunity by modulating IFN-beta production. *J Exp Med*. 2009;206(5):1167–1179.
36. Chessler AD, Ferreira LR, Chang TH, Fitzgerald KA, Burleigh BA. A novel IFN regulatory factor 3-dependent pathway activated by trypanosomes triggers IFN-beta in macrophages and fibroblasts. *J Immunol*. 2008;181(11):7917–7924.
37. Hintze KJ, Theil EC. DNA and mRNA elements with complementary responses to hemin, antioxidant inducers, and iron control ferritin-L expression. *Proc Natl Acad Sci U S A*. 2005;102(42):15048–15052.
38. Marro S, et al. Heme controls ferroportin1 (FPN1) transcription involving Bach1, Nrf2 and a MARE/ARE sequence motif at position -7007 of the FPN1 promoter. *Haematologica*. 2010;95(8):1261–1268.
39. Larson JA, Howie HL, So M. *Neisseria meningitidis* accelerates ferritin degradation in host epithelial cells to yield an essential iron source. *Mol Microbiol*. 2004;53(3):807–820.
40. Das NK, Biswas S, Solanki S, Mukhopadhyay CK. *Leishmania donovani* depletes labile iron pool to exploit iron uptake capacity of macrophage for its intracellular growth. *Cell Microbiol*. 2009;11(1):83–94.
41. Breuer W, Shvartsman M, Cabantchik ZI. Intracellular labile iron. *Int J Biochem Cell Biol*. 2008;40(3):350–354.
42. Liu XB, Nguyen NB, Marquess KD, Yang F, Haile DJ. Regulation of hepcidin and ferroportin expression by lipopolysaccharide in splenic macrophages. *Blood Cell Mols Dis*. 2005;35(1):47–56.
43. Theurl I, et al. Autocrine formation of hepcidin induces iron retention in human monocytes. *Blood*. 2008;111(4):2392–2399.
44. Lee GT, et al. Induction of interleukin-6 expression by bone morphogenetic protein-6 in macrophages requires both SMAD and p38 signaling pathways. *J Biol Chem*. 2010;285(50):39401–39408.
45. Portugal S, et al. Host-mediated regulation of superinfection in malaria. *Nat Med*. 2011;17(6):732–737.
46. Poss KD, Tonegawa S. Heme oxygenase 1 is required for mammalian iron reutilization. *Proc Natl Acad Sci U S A*. 1997;94(20):10919–10924.
47. Kovtunovych G, Eckhaus MA, Ghosh MC, Ollivierre-Wilson H, Rouault TA. Dysfunction of the heme recycling system in heme oxygenase 1 deficient mice: effects on macrophage viability and tissue iron distribution. *Blood*. 2010;116(26):6054–6062.
48. Murray HW. Pretreatment with phorbol myristate acetate inhibits macrophage activity against intracellular protozoa. *J Reticuloendothel Soc*. 1982;31(6):479–487.
49. Nathan C, Nogueira N, Juangbhanich C, Ellis J, Cohn Z. Activation of macrophages in vivo and in vitro. Correlation between hydrogen peroxide release and killing of *Trypanosoma cruzi*. *J Exp Med*. 1979;149(5):1056–1068.
50. McCabe RE, Mullins BT. Failure of Trypanosoma cruzi to trigger the respiratory burst of activated macrophages. Mechanism for immune evasion and importance of oxygen-independent killing. *J Immunol*. 1990;144(6):2384–2388.
51. Munoz-Fernandez MA, Fernandez MA, Fresno M. Activation of human macrophages for the killing of intracellular *Trypanosoma cruzi* by TNF-alpha and IFN-gamma through a nitric oxide-dependent mechanism. *Immunol Lett*. 1992;33(1):35–40.
52. Metz G, Carlier Y, Vray B. *Trypanosoma cruzi* upregulates nitric oxide release by IFN-gamma-preactivated macrophages, limiting cell infection independently of the respiratory burst. *Parasite Immunol*. 1993;15(12):693–699.
53. Dhiman M, Garg NJ. NADPH oxidase inhibition ameliorates *Trypanosoma cruzi*-induced myocarditis during Chagas disease. *J Pathol*. 2011;225(4):583–596.
54. Guevara AG, Guilvard E, Borges MM, Cordeiro da Silva A, Ouaissi A. N-Acetylcysteine and glutathione modulate the behaviour of *Trypanosoma cruzi* experimental infection. *Immunol Lett*. 2000;71(2):79–83.
55. Monteiro MC, et al. N-acetyl-L: -cysteine reduces the parasitism of BALB/c mice infected with *Leishmania amazonensis*. *Parasitol Res*. 2008;102(4):801–803.
56. Wilson ME, Andersen KA, Britigan BE. Response of *Leishmania chagasi* promastigotes to oxidant stress. *Infect Immun*. 1994;62(11):5133–5141.
57. Lima MF, Villalta F. *Trypanosoma cruzi* receptors for human transferrin and their role. *Mol Biochem Parasitol*. 1990;38(2):245–252.
58. Loo VG, Lalonde RG. Role of iron in intracellular growth of *Trypanosoma cruzi*. *Infect Immun*. 1984;45(3):726–730.
59. Arantes JM, et al. *Trypanosoma cruzi*: treatment with the iron chelator desferrioxamine reduces parasitemia and mortality in experimentally infected mice. *Exp Parasitol*. 2007;117(1):43–50.
60. Lalonde RG, Holbein BE. Role of iron in *Trypanosoma cruzi* infection of mice. *J Clin Invest*. 1984;73(2):470–476.
61. Shan Y, Zheng J, Lambrecht RW, Bonkovsky HL. Reciprocal effects of micro-RNA-122 on expression of heme oxygenase-1 and hepatitis C virus genes in human hepatocytes. *Gastroenterology*. 2007;133(4):1166–1174.
62. Zhu Z, et al. Heme oxygenase-1 suppresses hepatitis C virus replication and increases resistance of hepatocytes to oxidant injury. *Hepatology*. 2008;48(5):1430–1439.
63. Crespo I, et al. Melatonin prevents the decreased activity of antioxidant enzymes and activates nuclear erythroid 2-related factor 2 signaling in an animal model of fulminant hepatic failure of viral origin. *J Pineal Res*. 2010;49(2):193–200.
64. Santello FH, et al. Melatonin treatment reduces the severity of experimental *Trypanosoma cruzi* infection. *J Pineal Res*. 2007;42(4):359–363.
65. Gong P, et al. Activation of the mouse heme oxygenase-1 gene by 15-deoxy-Delta(12,14)-prostaglandin J(2) is mediated by the stress response elements and transcription factor Nrf2. *Antioxid Redox Signal*. 2002;4(2):249–257.
66. Rodrigues WF, Miguel CB, Chica JE, Napimoga MH. 15d-PGJ(2) modulates acute immune responses to *Trypanosoma cruzi* infection. *Mem Inst Oswaldo Cruz*. 2010;105(2):137–143.
67. Nagajyothi F, Zhao D, Weiss LM, Tanowitz HB. Curcumin treatment provides protection against *Trypanosoma cruzi* infection [published online ahead of print January 4, 2012]. *Parasitol Res*. doi:10.1007/s00436-011-2790-9.
68. Yet SF, et al. Hypoxia induces severe right ventricular dilatation and infarction in heme oxygenase-1 null mice. *J Clin Invest*. 1999;103(8):R23–R29.
69. Itoh K, et al. An Nrf2/small Maf heterodimer mediates the induction of phase II detoxifying enzyme genes through antioxidant response elements. *Biochem Biophys Res Commun*. 1997;236(2):313–322.
70. Livak KJ, Schmittgen TD. Analysis of relative gene expression data using real-time quantitative PCR and the 2(-Delta Delta C(T)) Method. *Methods*. 2001;25(4):402–408.